Energy Equip. Sys. / Vol. 13/No. 1/March 2025/ 15-33

ENERGY EQUIPSYS

Energy Equipment and Systems

www.energyequipsys.com

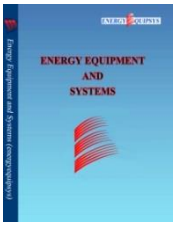

Investigating the effect of diamond-shape turbulator in optimal design of flat plate solar collector

Manuscript Type
Research Paper

Authors

Hassan Hajabdollahi [a]
Mohammad Shafiey Dehaj [a]
Farzaneh Hajabdollahi [b*]

[a] Department of Mechanical Engineering, Vali-e-Asr University of Rafsanjan, Rafsanjan, Iran

[b] Department of Mechanical Engineering, University of Colorado Denver, 1200 Larimer street, Colorado, 80217, U.S.A

Article history:

Received: 6 August 2024
Revised: 14 October 2024
Accepted: 1 November 2024

ABSTRACT

Operation of flat plate solar collector (FPSC) at the optimal point with maximum efficiency is very significant. Therefore, the optimum design of FPSC considering a diamond-shape turbulator (DST) is investigated. Six design parameters associated with the FPSC as well as two parameters for DST, including cone angle and tail length ratio, are considered as eight decision variables. Then, optimization is performed by selecting thermal efficiency and total annual cost (TAC) as objective functions and their results are assessed with the optimum design of a collector with plain tube. The results show that better thermos-economic results is found by the application of DST compared with a plain tube for an efficiency higher than 0.5566 while the use of a plain tube is more beneficial for an efficiency lower than 0.5566. Optimization is also performed for the higher electricity price and results reveal that in some higher electricity prices, the use of tube with DST is not beneficial for the all range of efficiency compared with plain tube. The results showed that the lower thickness of the bottom insulator is necessary for the model of DST in contrast to the plain tube. The higher cone angle and lower tail length ratio lead to the higher collector efficiency.

Keywords: Flat Plate Collector; Diamond-Shape Turbulator; Plain Tube; Thermo-Economic Pptimization; Pareto Front.

1. Introduction

Solar systems are a kind of heat exchanger where the solar radiation is transferred to the interior energy of the working fluid. Collectors are an essential part of the solar system. Actually, a collector is a device that engrosses the sun's incoming radiation and changes it to heat [1]. FPSCs are one of the most efficient and clean heating systems accessible [2]. This absorbed heat is then transferred by the working fluid for example oil, water, air or nanofluids where it flows in the FPSC. This absorbed energy is either transformed unswervingly into hot water through a working fluid or converted to air conditioners for convenience. Moreover, this deposited energy can be kept in a heat storage tank to be applied for different purposes at night or during cloudy weather [3].

Numerous procedures to enhance the solar collector efficiency for example the application of metal oxide nanofluids, inconstant tilt angles, and varying of volume flow rates applied [4]. Improvement in the FPSC efficiency is essentially due to decreased specific heat of working fluids [5]. But, in the solar systems, the

* Corresponding author: Farzaneh Hajabdollahi
Department of Mechanical Engineering, University of Colorado Denver, 1200 Larimer street, Colorado, 80217, U.S.A
E-mail address: farzaneh.hajabdollahiouderji@ucdenver.edu

efficiency is significantly influenced by the flow dispersion among the riser pipes [6-8].

In the FPSCs, the efficiency is powerfully related to the flow distribution dispersion among the riser pipes, in which an unvarying dispersion leads to a constant temperature scattering and consequently a higher thermal performance. García-Guendulain et al. [9] using the commercial software FLUENT® carried out numerical analysis. They concluded the flow scattering, pressure loss and consequently the performance of FPSC with flow dispersion in the plates inside the manifolds.

Khorasani-zadeh et al. [10] firstly, based on the experimental data, exergy analysis of the FPSC in a closed path and then the effect of using top, bottom, and side reflectors as well as their simultaneous application with a lens. Finally, based on a mathematical model, they optimized exergy in all situations. Hall et al. [11] studied the exergy of space solar receivers, assuming that the overall coefficient of heat loss depends on the power of the average outer surface temperature. Mahanta and Kumar [12] optimized the thermodynamics of flat plate collectors based on the minimized entropy produced. Torres Ries et al. [13] found the optimal fluid temperature and path length of the fluid flow for an overhead plate collector using dimensional relationships. Farhat et al. [14] studied the topic of exterior optimization of FPSCs. His work and most of the previous studies were performed assuming the total coefficient of heat loss of FPSC to be constant, and the exergy of the collector was expected to be the same to the initial temperature of the FPSC at environment temperature in an open circuit. The solar collector exergy examination is parametrically related to its energy and optical efficiency. The study and efficiency calculation of a FPSC using SiO2 nanofluid as an absorbing medium has been evaluated from the viewpoint of exergy, energy, energetic, economic, and ambient by Faizal et al. [15]. Harkouss et al. [16] conducted an optimization methodology for NZEB design by applying NSGA-II algorithm as the multi-objective optimization approach. Jani et al. [17] carried out a review on using of solar energy in hybrid desiccant cooling. They presented the newest findings on latest improvements in air-conditioning and the constructed ambient. Zhou et al [18] presented multivariable optimization for the optimum scheme and performance of the new solar system for the renewable energy cascade utilization.

Shafiey and hajabdollahi [19] carried out an optimization of a hybrid system with hourly evaluation through a year for various towns of Iran with different varieties of several parameters such as wind velocity, solar radiation, and temperature of ambient. They determined two concurrent objective functions, and applied a particle swarm optimization algorithm for finding the optimal value of important variables. Thermo-economic optimization of a refrigeration cycle was carried out by NSGA-II algorithm to get the best out of the COP and lowest the TAC by Hajabdollahi and Shafiey [20]. They found that COP and the TAC enhanced by growth in the percent of R32. Bezaatpour and Rostamzadeh [21] enhanced the Convection mechanism of FPSC by using rotary tubes, magnetic field inducer, and nanofluid. They showed that the Simultaneous installation of rotating pipes and magnetic field inducers with nanofluid is more effective. Qiu et al. [22] suggested the two novel mirrors employed for FPSC not needing solar pursuing and comparatively investigated Three kinds of mirrors by theoretic and investigational procedures. They indicated that the influence of enhancing the heat-gathering capability/temperature is significant. Mohan et al. [23] by applying Statistical techniques such as DOE, MANOVA, and regression analysis modeled and validated a MFPC. The findings showed that MFPC is 10–12% more efficient than conventional FPSC. Majumdar et al. [24] developed a tractable vigorous scheme with Genetic Algorithm to evaluate and optimize the thermal efficiency of FPSC. They achieved optimal magnitudes and volume flow rates for assumed exit temperature and effectiveness.

A comprehensive study of the latest progress, procedures, vital commercial influences, the importance of FPSCs, and the analysis encountered by the applications of FPSCs, which could be valuable for all applications of solar energy provided by Sheikholeslami et al. [25]. Verma et al. [26] experimentally investigated a new plan and construction methodology which related to for evaluation of FPSC efficiency. They developed a new tube design of collector as compared to the oldest organization tubes linked with shots in usual kind of FPSC. The results indicated that thermal performance reached

21.94% in comparison with conventional FPSC design. Numerical thermoeconomic evaluation of integrated FPSC with applying the heat exchanger as solar collector was performed by Hajabdollahi [27]. He obtained The optimal values of 16 decision parameters. Vengadesan and Senthil [28] critically presented the latest studies on thermal efficiency improvement of the FPSCs considering the various and important parameters. They founded that the instability influence in the bottom layer enhances the rate of convection heat transfer. Ganjehkaviri and Jaafar [29] modeled and optimized the FPSC with constructal configuration. They carried out Multi-objective optimization by employing the PSO algorithm and considered efficiency and TAC as two main parameters. Their results indicated that the thermal efficiencies in the case of constructal higher than 0.54 in association to the usual model. Karki et al. [30] studied several climatic and design scenarios for FPSCs. They reported a new approach to evaluate possibility of developed solar systems. They also found that additional welfares of enhancing area of solar collector reduce because of great costs of installation. Visa et al. [31] developed A unique kind of triangle FPSC. According to the finding results, different collectors with various absorber plates were constructed and thermal performances enhanced. Ma et al. [32] design and optimized a new FPSC module. Results showed that heat recovery from condensation efficiently enhanced the production and consumption. Hajabdollahi et al. [33] optimized five different heat exchangers by employing four various algorithms involving RGA, DE, PSO and BGA. Concept of balance was used to improve the important parameters of the thermal systems by Hajabdollahi and Shafiey [34].

Cetina-Quiñones et al. [35] mathematically modeled FPSC by applying different PCMs. They assessed an economic evaluation in two regions, industrial and residential. Also, they gained a maximum IRR of 22% for the residential sector. Dong et al. [36] considered a unique model of FPSC. They claimed that the design concept reduced the costs of installation of solar systems. The findings illustrated that the new design of FPSC carried out greater efficiency than the older one. Balaji et al. [37] performed a novel study of mixed convection influences of FPSC to increase effectiveness of absorber tube and evaluation was carried out among them for similar working conditions. They observed The major decrease in Richardson number for rod and tube FPSC. Anirudh and Dhinakaran [38] investigated the effect of the variation of two parameters on the performance and efficiency of FPSC with different foam permeability values. They performed Performance analysis to propose optimum parameter ranges of FPSC with porous foam. Hajabdollahi et al. [39] studied a novel arrangement to increase of air temperature based on solar energy. Also, solar heater by employing FPSCs is studied and optimized by Hajabdollahi et al. [40]. Their findings revealed that it was not important effect on performance of FPSC. Dhairiyasamy et al. [41] tried to enhance FPSC performance using internal barrier optimization technique. They also fabricated test apparatus to calculation different collectors with one-four barriers under stable settings. Ghalati et al. [42] optimized and estimated thermal performance of FPSC by employing ANN and RSM algorithm. They founded that FPSC performance with porous plate is more than simple plate by 42%. The new design of a Y-shaped duct nerwork for FPSC is provided by Ojead et al. [43]. They used a power low nanofluid with several volume fractions as working fluid. Li et al. [44] optimized the flow channel of FPSC by applying theory of field synergy. They enhanced the FPSC performance by employing S-bend flow channel.

To enhance the efficiency of the FPSC, this study introduces a novel approach: the integration of a diamond-shaped turbulator (DST) into the tube side. This method aims to increase rates of heat transfer while maintaining a moderate pressure drop increase. While DSTs can improve Nusselt numbers, they also lead to higher pumping power, raising questions about their overall benefit. To address this, our research focuses on thermo economic modeling and optimization of the FPSC with DST integration. The goal is to maximize efficiency while minimizing the TAC. Given the inherent conflict between efficiency and cost, we employ optimization techniques with a multi-objective function to balance both parameters. Eight important parameters are considered, including six design parameters for the FPSC and two for the DST (cone angle and tail length ratio). At the end, they are the novelty of the present work on the topic:

- Flat-plate solar collector is thermo-economically modeled and optimized.
- Multi-objective optimization is carried out evaluating TAC and efficiency as objective functions.
- As novelty, diamond shape turbulator is applied to improve the heat transfer rate.
- Optimization is performed in two general cases including a collector with turbulator and without turbulator.
- Eight important variables involving number and diameter of tube, length and width of panel, bottom and lateral of insulator thickness, insulator as well as turbulator tail length ratio and cone angle are considered.

Numerical

A_p	surface area (m2)
b	space between tubes (m)
C_b	bond resistance
C_p	heat capacity (J kg-1 K-1)
C_{col}	collector investment cost ($)
C_{inv}	annual cost of investment ($ year-1)
C_{op}	annual cost of operation ($ year-1)
C_{pump}	pump investment cost ($)
C_t	total annual cost ($ year-1)
D	tube diameter (m)
D_i	tube inner diameter (m)
D_o	tube outer diameter (m)
f	friction factor (–)
F_R	effectiveness removal factor (–)
h	convection heat transfer coefficient (W2 m-2 K-1)
h_{fi}	tube side convection heat transfer coefficient (W2 m-2 K-1)
I	solar radiation intensity (W2 m-2)
I_T	solar radiation incident on the tilted collector
I_b	beam radiation
I_d	sky diffuse radiation
I_r	ground-reflected solar radiation
k	conductivity (W2 m-1 K-1)
k_{el}	price of electrical energy ($ kWh-1)
l	third root of V
L	panel length (m)
t_{li}	Lateral insulator thickness (m)
t_{bi}	Bottom insulator thickness(m)
$\dot{m}$	mass flow rate (kg s-1)
N_t	number of tube
Nu	nusselt number
N_h	hours of operation (hour year-1)
N_c	number of cover $(-)$
Nu	Nusselt number $(-)$
i	interest rate $(-)$
Pr	prandtl number
$\dot{Q}_u$	useful heat energy gain (W)
Ra	Rayleigh number
TR	tail length ratio (l_t/l_h)
Re	Reynolds number $(-)$
s	system life
t	thickness (m)
T_a	ambient temperature (^oC)
T_b	bulk temperature (^oC)
T_p	absorber's plate temperature (^oC)
T_i	collector inlet temperature (^oC)
T_{out}	collector outlet temperature (^oC)
U	collector loss coefficient (W2 m-2 K-1)
V	collector structure volume (m^3)
$\vec{V}$	velocity (m/s)
t_{p-c}	space between plate and cover (m)
W	panel width (m)
$\dot{W}_p$	pump power (kW)
Y	yearly cost coefficient (year)

Greek Letter

ε	emissivity $(-)$
τ	transmittance $(-)$
α	absorptance $(-)$
$(\tau\alpha)$	effective optical fraction
η	collector efficiency $(-)$
η_F	fin efficiency $(-)$
η_p	pump efficiency $(-)$
μ	viscosity (Pa.s)
σ	Stefan–Boltzmann constant
ΔP	pressure drop (pa)
β	collector tilt (°)
θ	included cone angle (°)
$\forall_{insu}$	insulation volume (m^3)
δ	fin thickness (m)

ρ_g	reflectance from the surroundings (–)

Subscripts

a	ambient
b	bottom
col	collector
e	edge
eff	effective
f	Fluid
insu	insulation
p	plate
p-c	plate- cover
r	radiation
t	top

2. Thermo-economic modeling

To optimize FPSC by considering the thermo-economic aspect needs a thermodynamic and TAC model. Forecasting of PTSC efficiency regarding some thermodynamic variables was provided by the thermodynamic model, while the TAC model calculated cost values for an assumed set of the thermodynamic variables.

2.1. Theory of the FPSC efficiency

The optimization design of the FPSC is to gain the highest incident energy on a specified horizontal and constant FPSC of length panel × width panel. The main portion of this system is a flat plate. Figure 1 shows the FPSC with the details of a plain tube in the solar system and the tube with a diamond-shaped turbulator. The FPSC thermal performance can be indicated by the ratio of the suitable energy to the incident energy on the FPSC. FPSCs can gather diffuse solar radiation likewise direct solar radiation.

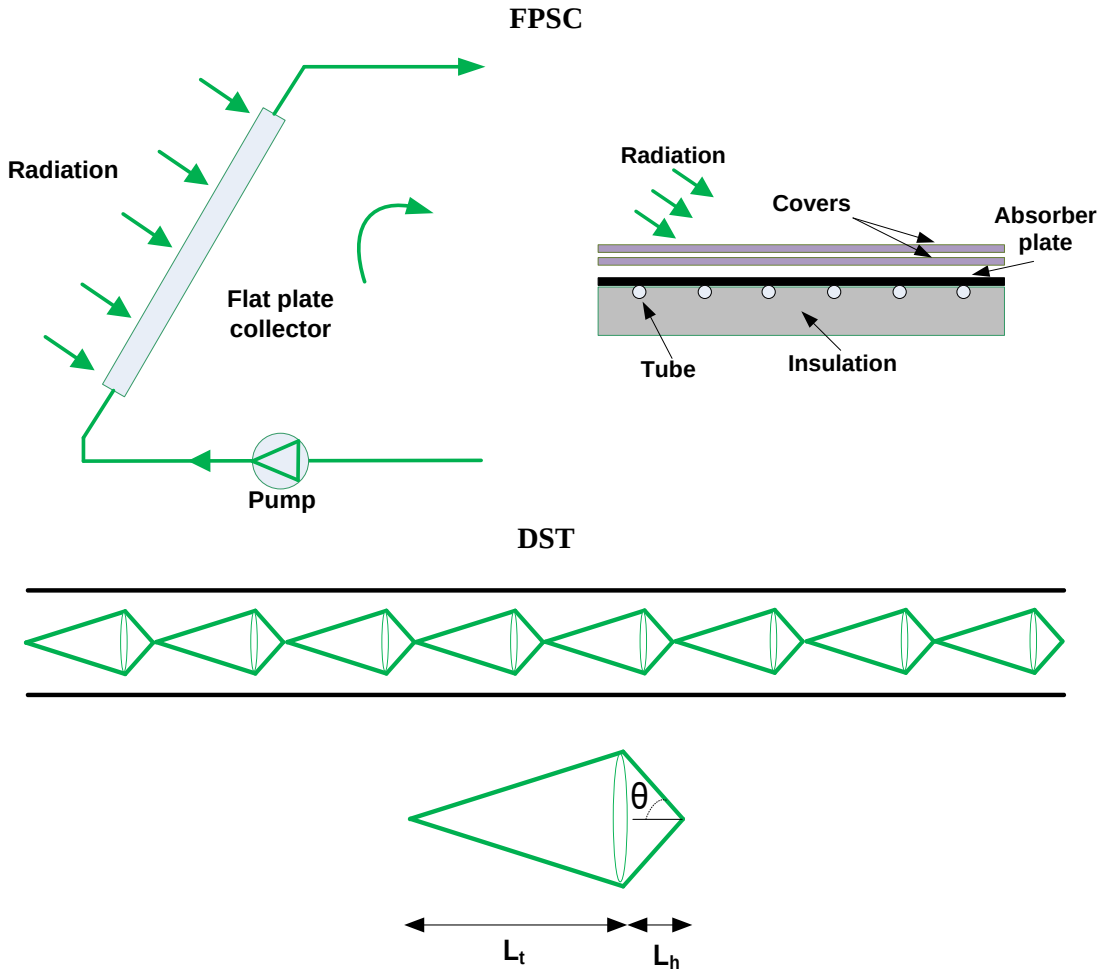

Fig. 1 FPSC Schematic diagram and tube with turbulator

For calculating and modeling the FPSC efficiency, the amount of the solar energy that is attracted by the absorbent plate of the solar collector is required. The incident radiation of solar energy on a sloped surface involves diffuse, beam and ground-mirrored radiation [45]. The beam and diffuse radiation will be mobile among the transparent shields. Transmittance improving of the solar collector glazing will outcome in additional radiation established by the absorbent plate. The radiation energy attracted by the plate can be calculated as below [46]:

$$\dot{Q}_{\mathrm{r}} = \dot{q}_{\mathrm{r}} A_{\mathrm{p}} = (\tau\alpha)_{\mathrm{eff}} I_{\mathrm{T}} A_{\mathrm{p}} \tag{1}$$

where $(\tau\alpha)$ is the actual optical fraction of the absorbed energy. In the above relation, I_T is total solar radiation which is aggregation of ground-reflected solar radiation (I_r), sky diffuse (I_d) and beam (I_b), and defined as below:

$$I_{\mathrm{T}} = I_{\mathrm{b}} + I_{\mathrm{d}} + I_{\mathrm{r}} \tag{2}$$

in addition, I_T can be evaluated by Hay et al. [47].

$$I_T = \left(I_b + I_d \frac{I_b}{I_h} \right) R_b + I_d \left(1 - \frac{I_b}{I_h} \right) \left(\frac{1+\cos\beta}{2} \right) \left(1 + \sqrt{I_b / I_h} \sin^3\left(\frac{\beta}{2} \right) \right) + I_h \rho_g \left(\frac{1-\cos\beta}{2} \right) \tag{3}$$

in which, β is the collector tilt. Commonly, FPSCs have excessive heat losses. The main aim of finishing is stopping infrared thermal energy to getaway. Though, the dissimilarity among the temperature of the absorbent plate and the environment temperature result in increasing the convective heat transfer to the ambient. This convective heat transfer can be considered as follow [46]:

$$\dot{Q}_{\mathrm{conv}} = \dot{q}_{\mathrm{conv}} A_{\mathrm{p}} = U A_{\mathrm{p}} \left(T_{\mathrm{p}} - T_{\mathrm{a}} \right) \tag{4}$$

where, A_p is collector surface area and U is collector loss coefficient. The rate of radiation heat losses can be determined by the below relation [46]:

$$\dot{Q}_{\mathrm{rad}} = \dot{q}_{\mathrm{rad}} A_{\mathrm{p}} = \varepsilon_{eff} \sigma A_{\mathrm{p}} \left(T_{\mathrm{p}}^4 - T_{\mathrm{a}}^4 \right) \tag{5}$$

In the above equation, ε_{eff}, σ and T_p are effective emission, constant of Stefan–Boltzmann and temperature of absorber's plate, respectively. Because of the insulation of collector bottom and the collector edges, heat losses are very low and can be ignored. By combination Eqs. (1), (4) and (5), the valuable energy can be obtained as:

$$\dot{Q}_{\mathrm{u}} = \dot{q}_{\mathrm{u}} A_{\mathrm{p}} = (\tau\alpha)_{\mathrm{eff}} I_{\mathrm{T}} A_{\mathrm{p}} - U A_{\mathrm{p}} \left(T_{\mathrm{p}} - T_{\mathrm{a}} \right) - \varepsilon_{eff} \sigma A_{\mathrm{p}} \left(T_{\mathrm{p}}^4 - T_{\mathrm{a}}^4 \right) \tag{6}$$

Additionally, the suitable energy (heat) of the working fluids can be obtained by the following relation [47]:

$$\dot{Q}_{\mathrm{u}} = \dot{m} C_{\mathrm{p}} \left(T_{\mathrm{out}} - T_{\mathrm{in}} \right) \tag{7}$$

where, T_{in} is temperature of inlet and T_{out} is the temperature of the outlet of the collector, respectively. The FPSC efficiency (η) can be evaluated as:

$$\eta = \frac{\dot{Q}_{\mathrm{u}}}{I_{\mathrm{T}} A_{\mathrm{p}}} \tag{8}$$

To communicate the real collector efficiency directly and in temperature aspects of the valuable energy from the fluid movement in a closed circuit, the thermal performance and the valuable heat can be determined from:

$$\eta = F_{\mathrm{R}} \left[(\tau\alpha)_{\mathrm{eff}} - \frac{U A_{\mathrm{p}} \left(T_{\mathrm{p}} - T_{\mathrm{a}} \right)}{I_{\mathrm{T}} A_{\mathrm{p}}} \right] \tag{9}$$

Additionally, heat removal factor (F_R) obtained as:

$$F_R = \frac{\dot{m} c_p}{A_c U} \left[1 - \exp\left(- \frac{A_c U F'}{\dot{m} c_p} \right) \right] \tag{10}$$

so, F' is:

$$F' = \frac{1/U}{W \left(\frac{1}{U \left[D_o + (b - D_o) \eta_F \right]} + \frac{1}{C_b} + \frac{1}{\pi D_i h_{fi}} \right)} \tag{11}$$

h_{fi} is the coefficient of convective heat transfer in the tube side and the details for various ranges of Reynolds number (Re) are stated in references [48, 49]. Additionally, fin efficiency (η_F) with rectangular shape obtained as below:

$$\eta_F = \frac{\tanh\left[m (b - D_o)/2 \right]}{m (b - D_o)/2}, \quad m = \sqrt{U_L / (k\delta)} \tag{12}$$

In the above relation, b, D_0 and δ are space between tubes, tube outer diameter and fin thickness, respectively. The coefficient of general loss (U) of the FPSC is a summation of lowest, top and edge lost coefficients expressed as:

$$U = U_b + U_e + U_t \tag{13}$$

where U_b, U_e and U_t calculated from Eqs. (14), (15) and (16) respectively:

$$U_b = (k/t)_{insu,b} \tag{14}$$

$$U_e = (k/t)_{insu,e}(A_c/A_e) \tag{15}$$

$$U_t = 1/\left(R_1 + \sum_{i=1}^{N_c} R_{2,i}\right) \tag{16}$$

in Eq. (16), R_1 and R_2 obtained as follow [50, 51]:

$$R_1 = 1/\left([\varepsilon_c \sigma (T_c^2 + T_a^2)(T_c + T_a)] + \max\left(5, 8.6\frac{V^{0.6}}{l^{0.4}}\right)\right) \tag{17}$$

$$R_2 = 1/\left([\frac{\sigma (T_p^2 + T_c^2)(T_p + T_c)}{1/\varepsilon_p + 1/\varepsilon_c - 1}] + [\frac{Nu_a k_a}{t_{p-c}}]\right) \tag{18}$$

It should be noted that, Nu_a is an ambient Nusselt number which is a function of tilt angles (from 0 to 75º) and Raleigh number [52]. Generally, the Nusselt number can be deliberate as follows [46]:

$$Nu = \frac{hD}{k} \tag{19}$$

in which, the coefficient of convective heat transfer (h) can be obtained by using the below function:

$$h = \frac{\dot{Q}_u}{A_p(T_p - T_b)} \tag{20}$$

here T_b is the bulk temperature and is determined as:

$$T_b = \frac{T_{in} + T_{out}}{2} \tag{21}$$

where Nusselt number for both case of plain tube and tube with DST are obtained as follows respectively [52]:

$$Nu = 0.02\,\mathrm{Re}^{0.8}\,\mathrm{Pr}^{0.4} \tag{22}$$

$$Nu = 0.105\,\mathrm{Re}^{0.676}(\tan\theta)^{0.135}\mathrm{Tr}^{-0.214}\,\mathrm{Pr}^{0.4} \tag{23}$$

where TR is the diamond tail length ratio (l_t/l_h) as depicted in Fig. 1. In addition, Re and Pr are Reynolds and Prandtl numbers, respectively, and determined as below:

$$\mathrm{Re} = 4\dot{m}/(\pi D_i \mu N) \tag{24}$$

$$\mathrm{Pr} = \frac{C_p \mu}{k} \tag{25}$$

In which, the pressure drop (ΔP) is assessed from below equation:

$$\Delta p = f\frac{L}{d}\frac{\rho\vec{V}^2}{2} + \sum K\rho\frac{\vec{V}^2}{2}, \tag{26}$$

In the above relation, $\sum K$ is the aggregation of the coefficients of local loss and the velocity of the fluid can be gained as:

$$\vec{V} = \frac{\dot{m}}{\rho A},\ A = \pi d^2/4 \tag{27}$$

The friction factor (f) for both cases of plain tube and tube with DST are obtained as follows respectively [53]:

$$f = 1.19\,\mathrm{Re}^{-0.375} \tag{28}$$

$$f = 2.7\,\mathrm{Re}^{-0.263}(\tan\theta)^{0.143}TR^{-.291} \tag{29}$$

It is indicated that the Eq. (23) and Eq. (29) are valid for angles in the range of 15-45º and tail length ratio in the range of 1-2.

2.2. Economic parameter

Another significant parameter in optimal design of the FPSC is TAC containing sum of operating and investment cost (electricity price for pumping) which is estimated as follow:

$$C_t = Y C_{inv} + C_{op} = \phi\left\{\begin{matrix} a_1(N_t)^{b_1} + a_2(D_{tube})^{b_2} + a_3(L)^{b_3} \\ +a_4(W)^{b_4} + a_5(t_{li})^{b_5} + a_6(t_{bi})^{b_6} + \end{matrix}\right\} + a_7\dot{W}_p^{\,b_7} \tag{30}$$

in fact, the cost of investment involved the capital cost of FPSC such as absorber plate area (L×W), outside area of tubes ($N_t \times \pi D$), insulator volume (a function of surface area and insulator thickness), and cost of assemblage (φ). On the other hand, operational cost is related to the required power for pumping. Furthermore, a_1 *to* a_7 and b_1 *to* b_7 are fixed coefficients according to the existing market price of the apparatus. It is noticed that coefficients of a, b and assembly factor of collector in Eq. (30) are likewise supposed to be [120 60 220 4.5 30 30 3500], [0.9 0.8 1 1 1 1 0.47] and 1.5, respectively according the market existing price [49].

Y is the coefficient of yearly cost expressed as:

$$Y = \frac{i}{1-(1+i)^s} \tag{31}$$

therefore, i and s are the rate of interest and life of the system, respectively. The power for fluid pumping (pumping power; $\dot{W}$) can be determined by Eq. 32 [54]:

$$\dot{W} = \left(\frac{\dot{m}}{\rho}\right)\Delta p \quad (32)$$

Finally, the cost of pumping power operating to conquer the pressure loss (ΔP) in the pipes estimated as follows:

$$C_{op} = k_{el} N_h \dot{W} \quad (33)$$

2. 3. Solution procedure

As the radiation resistances depend on the plate of the absorber and the temperature of cover, the solution procedure requires a practice of try and error as presented in below:

1. The plate of the absorber and the temperature of the cover is predicted.
2. The heat transfer rate is measured by the description of total loss coefficient of collector, physical condition and absorbed radiation of FPSC such as number and diameter of tube, volume flow rate, width and length of collector, thickness of insulator, transmission absorbance creation of absorber plate, etc.
3. At that time, the temperature of cover is revised by following equation:

$$T_c = T_p - R_2 U_t (T_p - T_a) \quad (34)$$

4. The predicted temperature of cover is substituted by the newest temperature of cover and this procedure is reiterated from step 3 up to the merging is happened.
5. So, the temperature of plate is revised by below equation:

$$T_p = T_a + (S - \dot{Q}/A_c)/U_L \quad (35)$$

6. As the temperature of cover is calculated, the predicted temperature of plate is substituted by the newest one and this procedure is reiterated from step 2 until the merging is happened.
7. When the temperature of plate and temperature of cover are acquired, the heat transfer rate and FPSC performance are also obtained.

For better understanding of the procedure of optimization and modeling, the flowchart of is introduced in Fig. 2.

3. Findings and evaluation

3.1. confirmation of the present model

In the present investigation, a confirmed code which was before established by the author is used for thermal and economic evaluation of FPSCs [55].

3.2. Case study

The optimum design of the collector is carried out for Rafsanjan city located in the north of Kerman one of the southern provinces of Iran. The latitude of this city is 32^o and to absorb the maximum radiation, the collector angle to the horizon is also considered to be 32^o. Hourly analysis for solar radiation is performed considering the above assumptions and average radiation during a year is obtained (253Wm-2) and considered for modeling. Distilled water as working fluid (0.2 kg/s) comes into the collector at 20^{o}C whereas the temperature of the environment is supposed to be 10^{o}C. Additionally, the limitation is also defined to assure that the differences among temperature of water inlet and outlet of the FPSC is more than 1^{o}C. In other words, considering the water mass flow rate and heat capacity, the capacity of FPSC heat rate must be more than 0.84 kW. The economic input parameters including, interest rate, system life time and electricity price are considered to be 0.12, 15 years and 0.005 $ kWh-1, respectively. FPSC is optimized according to the design variables and variation of their ranges provided in Table. 1. In fact, six design variables involving diameter and number of tube, width and length of panel, thickness of bottom and lateral insulator are evaluated for a collector with plain tube while two additional parameters related to the turbulator (tail length ratio and cone angle) are added in the case of tube with DST. In fact, the number of design parameters in the case of a plain tube is 6 while it is 8 in the case of a tube with DST [49].

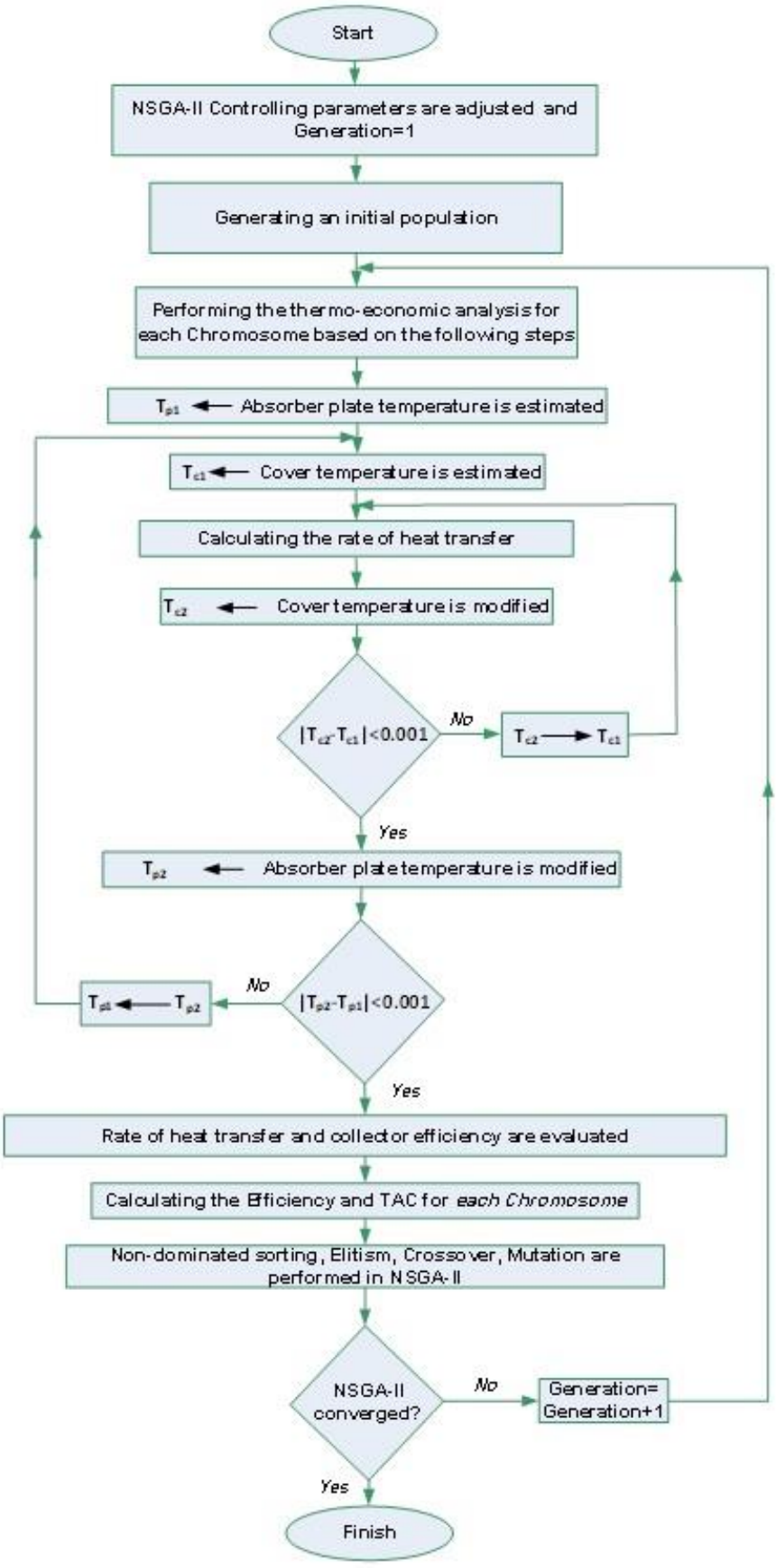

Fig. 2. optimization and modeling Flowchart

Table 1 decision variables and variation range of them

	Lower bound	**Upper bound**
Number of Tube (-)	2	50
Diameter of Tube (m)	0.005	0.03
Length of Panel (m)	0.5	4
width of Panel (m)	0.5	4
thickness of Lateral insulator (m)	0.02	0.05
thickness of Bottom insulator (m)	0.02	0.15
Tail length ratio (-)	1	2
Cone angle (^{o})	15	45

3.3. Optimization

To assess the optimal FPSC thermal efficiency with plain tubes and tubes fitted with DST, fast and elitism non-dominated genetic algorithm (NSGA-II) which was developed by Deb is used and coupled with modeling and developed for optimization [56-57]. NSGA-II's combination of efficiency, diversity preservation, and Pareto optimization makes it a strong choice for many multi-objective optimization problems [57]. In all considered subjects, a population size including 200 chromosomes has been determined with a crossover possibility of 80% and mutation possibility of 2% elitism parameter of 0.55. The two objectives in the present research including thermal performance and TAC should be balanced considering the design parameters listed in Table. 1. Therefore, the trend of the present optimization of FPSC can be expressed in the below:

$$\begin{cases} \text{maximize} & \eta = \text{Eq}\,(8) \\ \text{minimize} & \text{TAC} = \text{Eq}\,(30) \\ \\ \text{subject to} & \text{Design variables} \\ & \text{which presented in Table 1} \end{cases} \quad (36)$$

Figure 3 shows the optimal Pareto front for both studied cases (FPSC with DST and plain tube) with a minimum 0.84 kW as the rate of heat transfer. Therefore, the optimization program has been implemented four times for each case. Then, according to the non-dominated Pareto fronts, the Pareto fronts are combined simultaneously and the first ranked results are chosen as the final optimal Pareto front. According to the findings, it can be understood the two elected objective functions (TAC and efficiency) are opposed in the best state. Any work causes the increase of efficiency, result in an enhancement of the TAC and contrariwise. The multi objective optimization must be done to reveal the tendency of confliction in the optimal condition. The optimal TAC is improved by enhancing the FPSC effectiveness, however the slope of increase exceedingly improves for the highest possible efficiency. According to the Fig. 3, for both cases of plain tube and tube with DST the highest efficiency is at the design points A and *B* (0.5683 and 0.5717) respectively, whereas the TAC is the most expensive (296.6 and 294.1$ year-1) at these points. In other words, the lowest TAC for both cases of plain tube and tube with DST happens at design points I and H (263.8 and 266.2 $ year-1) respectively, while the minimum efficiency is 0.5340 and 0.5385. In fact, design points *A* and B are the optimal answer where the efficiency is the only objective function, whereas design points H and I are the optimum answer where the TAC is the only objective function.

As shown in Fig. 3, at point G the efficiency and TAC are the same for both cases of plain tube and tube with DST. Also, with the increase in efficiency from 0.5566 to 0.5717, the value of TAC in the item of plain tube is higher than the item of tube with DST. On the other hand, for the points with an efficiency below 0.5566, the TAC for the case of tube with DST is higher as compared with plain tube. It should be concluded that, FPSC with tube fitted with DST is dominated over the results of the plain tube for an efficiency higher than 0.5566 while the plain tube is a better thermos-economic trend for an efficiency lower than 0.5566. Additionally, the higher maximum efficiency was detected in the item of DST while the lower TAC in the item of the plain tube shows the advantage use of a tube with DST for the application of FPSC with higher efficiency and advantage use of plain tube for the application of FPSC with lower cost. Optimal quantities of two objectives for eight distinctive points from A to I (Pareto front) are provided, in Table. 2.

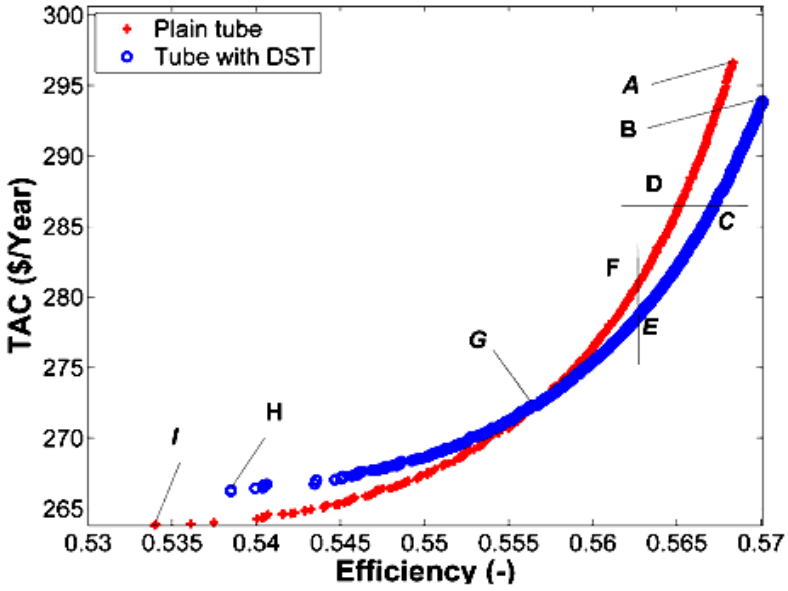

Fig. 3 Pareto optimal fronts for the collector with different tube geometry

Table 2 Optimal quantities of objective functions for points A-I in Fig. 3

Point	Thermal performance	TAC ($/year)
A	0.5683	296.6
B	0.5717	294.1
C	0.5672	286.3
D	0.5651	286.3
E	0.5626	278.5
F	0.5626	280.7
G	0.5566	272.2
H	0.5385	266.2
I	0.5340	263.8

To gain a suitable correlation for the finest decision of FPSC, the relation for FPSC TAC in terms of thermal performance for the both considered items are derivative for the Pareto front (Fig. 3) as follow:

$$C_{total}(\$/year)=\begin{pmatrix}5.323\eta_{col}^4-11.610\eta_{col}^3\\+9.492\eta_{col}^2-3.45\eta_{col}+0.4705\end{pmatrix}10^7 \quad (37)$$

$$C_{total}(\$/year)=\begin{pmatrix}7.271\eta_{col}^4-16.010\eta_{col}^3\\+13.230\eta_{col}^2-4.856\eta_{col}+0.6686\end{pmatrix}10^7 \quad (38)$$

The mentioned correlations are respectively valid for collectors with DST tube and plain tube.

3.4. Optimum design parameters

Table 3 shows the optimum design parameters of the collector with plain tube for five typical points in Fig. 3. According to the results listed in this table, the optimal quantity of tube number, tube diameter, and panel width for all optimum selected points are 24, 0.003 m and 2.59 m respectively.

Table 3 Optimal decision values for five typical points in Fig. 3 (collector with plain tube)

	A	D	F	G	H
Number of Tube (-)	24	24	24	24	24
Diameter of Tube (m)	0.003	0.003	0.003	0.003	0.003
length of Panel (m)	2.25	2.26	2.28	2.30	2.31
width of Panel (m)	2.59	2.59	2.59	2.59	2.69
Thickness of Lateral insulator (m)	0.050	0.050	0.050	0.049	0.049
Thickness of Bottom insulator (m)	0.150	0.124	0.109	0.085	0.047

In addition, the optimum design parameters of the collector with DST tube for five typical points in Fig. 3 are presented in Table. 4. As shown in this table, the optimum value of diameter and number of tubes and thickness of lateral insulator for all optimum selected points are 24, 0.003 m and 0.05 m respectively.

Variations of the design parameters related to the Pareto front can be operative and suitable in reaching the premium design settings. Figs. 4a-f shows the distribution selection of optimum design parameters versus the efficiency.

Table 4 Optimal decision variables for five typical points in Fig. 3 (collector with DST tube)

	B	C	E	G	I
Number of Tube (-)	24	24	24	24	24
diameter of Tube (m)	0.003	0.003	0.003	0.003	0.003
length of Panel (m)	2.25	2.25	2.27	2.25	2.28
width of Panel (m)	2.57	2.59	2.59	2.63	2.69
thickness of Lateral insulator (m)	0.050	0.050	0.050	0.050	0.050
Thickness of Bottom insulator (m)	0.150	0.115	0.094	0.077	0.048
Tail length ratio (-)	1.00	1.04	1.21	1.94	1.75
Cone angle (°)	44.9	44.7	41.5	41.6	15.9

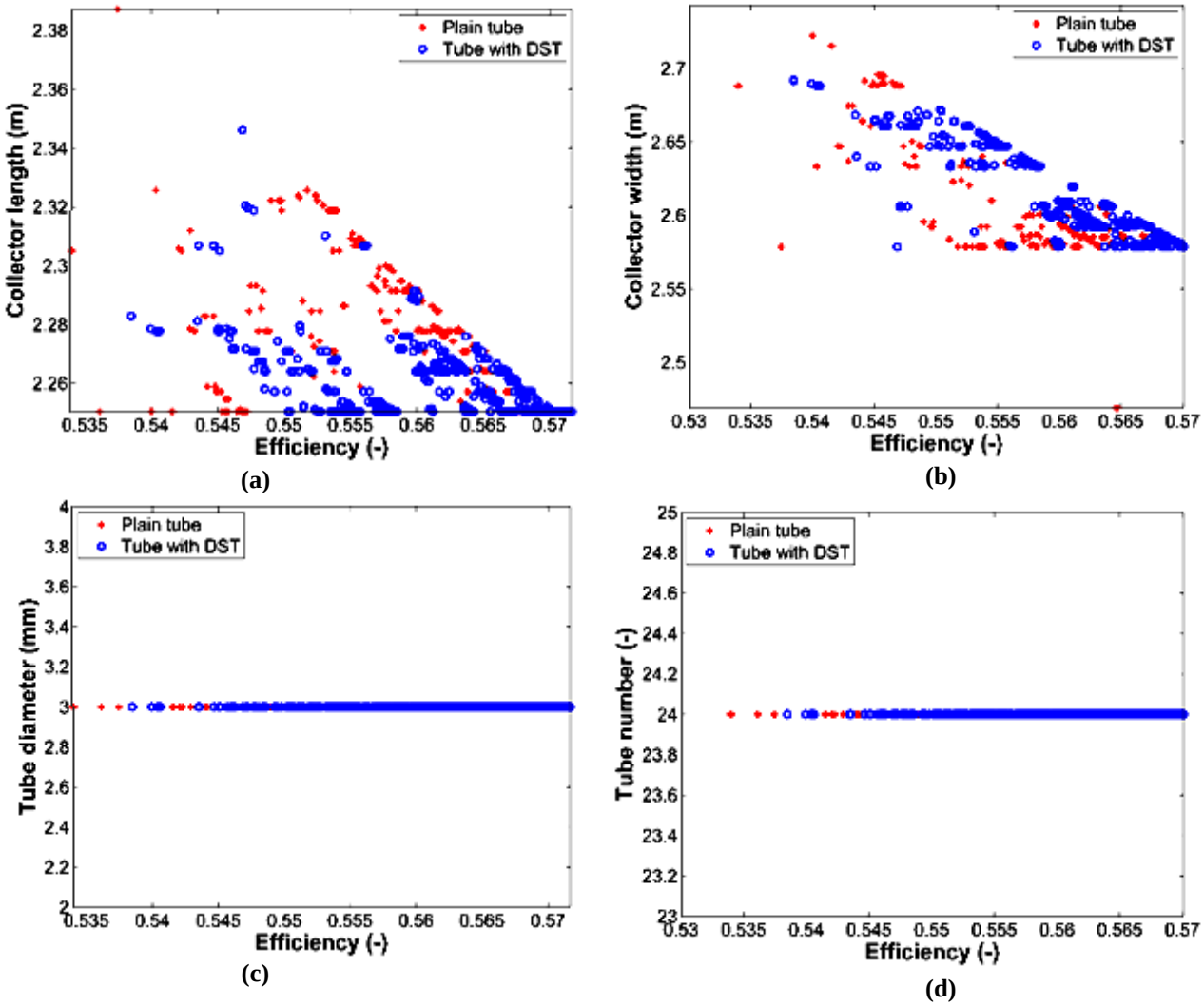

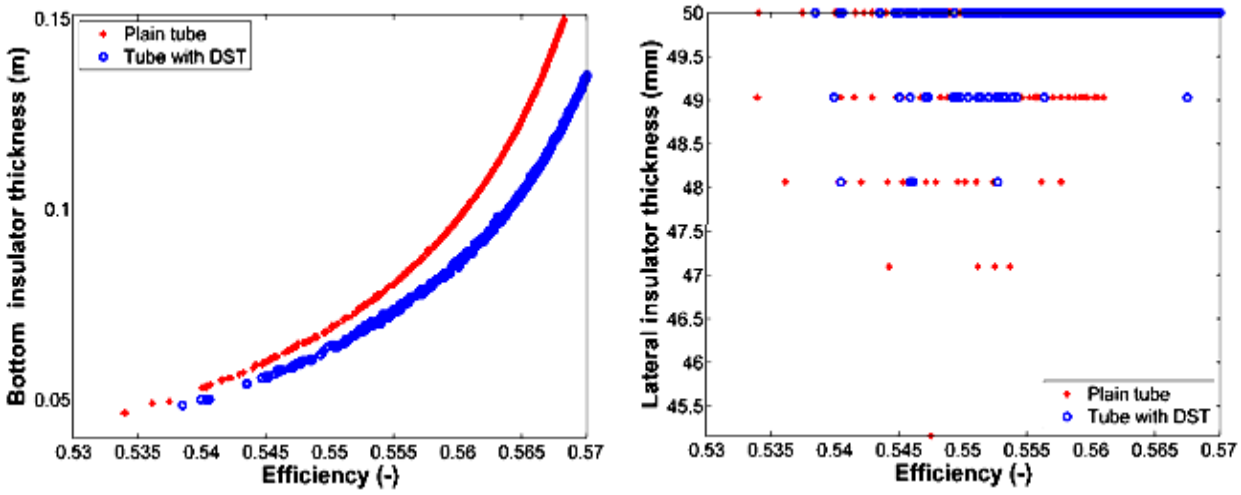

Fig. 4. Optimum design parameters versus efficiency for the points in Fig. 3. **a.** Collector length, **b.** Collector width, **c.** Tube diameter, **d.** Tube number, **e.** Bottom insulator thickness, **f.** Lateral insulator thickness

According to the results shown in Fig. 4a-b, at the same efficiency, the collector length of the plain tube is selected higher than the case of the tube with DST. Furthermore, to have a collector with optimum efficiency, the panel length for the case of the plain tube is selected in the range of 2.25-2.33 m. The mentioned range is 2.25-2.35 m in the case of the tube with DST. On the other hand, to have a collector with optimum efficiency, the panel width for the case of plain tube is selected in the range of 2.57-2.72 m. The mentioned range is 2.57-2.69 m in the case of the tube with DST. The findings in Figs. 4a-b reveal that efficiency improved in general by an increase of both collector length and width for both studied cases. The results in Figs. 4a-b also demonstrated that, generally the higher tube length and lower tube width are selected in the case of plain tube evaluated with the case of tube with DST. The optimum findings in Figs. 4c-d shows that the same and stable quantity of tube diameter and number are designated for both studied cases.

According to Fig. 4e at the same efficiency, the optimal quantity of thickness of the bottom insulator for case of the plain tube is selected higher than the tube with DST. The findings in this figure also prove that, a higher insulator thickness is required for the higher efficiency. In fact, for higher thermal efficiency, the rate of heat transfer should be modified. Using the higher insulator thickness causes lower heat loss and consequently higher rate of heat transfer and performance.

Finally, the distribution of lateral insulator thickness versus efficiency in Fig, 4f illustrates the selection of this parameter in the range of 45-50mm.

Distribution of turbulator variables involving cone angle and tail length ratio versus efficiency for the points in Fig. 3. Are represented in Figs. 5a-b. The findings in Figs. 5a-b demonstrates that both turbulator parameters are selected in their whole range of variation which shows the incompatible influence of these variables on objective functions. Actually, each quantity of selected variables could be deliberated as optimal which improves one objective function while destroying another one. For more details, the results in Figs. 5a-b shows that, the higher cone angle while the lower tail length ratio is required for higher efficiency. Based on the conflicting behavior of objective functions found in Fig. 3, it is predicted that the mentioned parameters have the reverse effect on TAC.

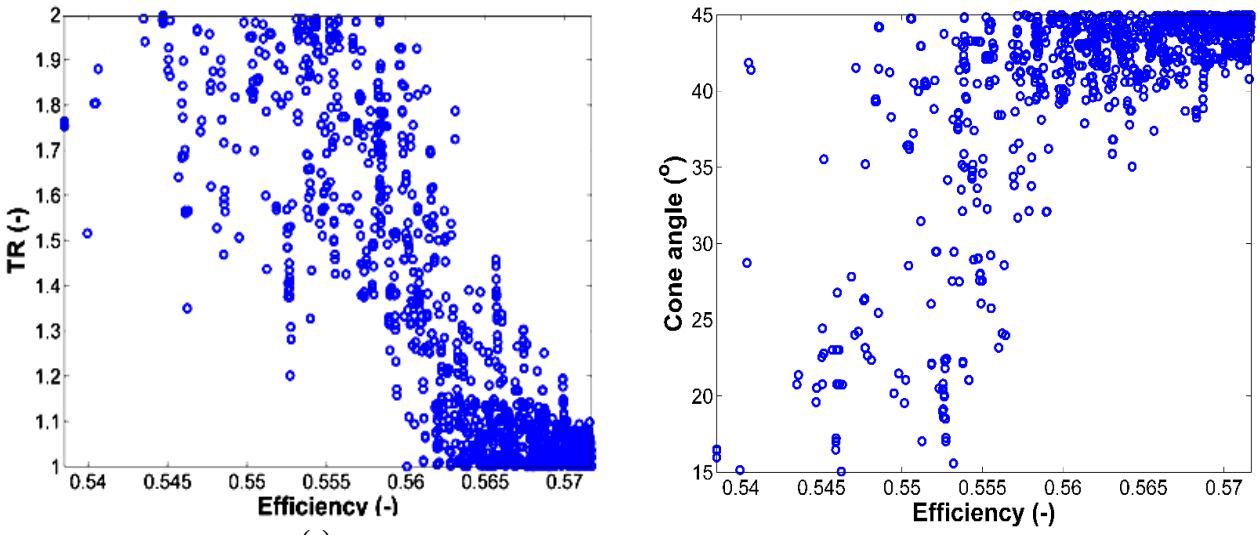

(a) (b)

Fig. 5 Optimum DST parameters versus efficiency for the points in Fig. 3. a. Cone angle, b. Tail length ratio

3.5. Electricity price

Applying a turbulator, increases the pressure drop and as a result the operational and general cost in the item of a tube with DST. On the other hand, electricity price affects the operational cost directly. As a result, the optimum results when the electricity price changes is desirable to investigate. For this purpose, optimum Pareto fronts for different electricity prices including 0.005, 0.01, 0.02, and 0.03 $ kWh-1 for two studied tube geometries are obtained and illustrated in Figs. 6a-b. The results in these figures for both studied cases reveal that the Pareto front with the higher electricity price is generally conquered by the results of the Pareto front with lower electricity price. The rate of domination is significantly higher in the case of tube with DST evaluated with plain tube (Fig. 6b versus Fig. 6a). To have a better understanding of the optimum results for both studied tube configurations, findings of Pareto fronts for different tube configuration are illustrated in Figs. 7a-c. As it can be seen, by increasing the electricity price, the value of marginal efficiency (efficiency in the intersection of two Pareto fronts) increases, and finally the tube with DST is not better than the plain tube for the all range of efficiency for the 0.03$kWh-1 as electricity price. The mentioned analysis reveals the importance of electricity price on the selection of any methods which increase both pressure drop and rate of heat transfer in the tube side of thermal systems.

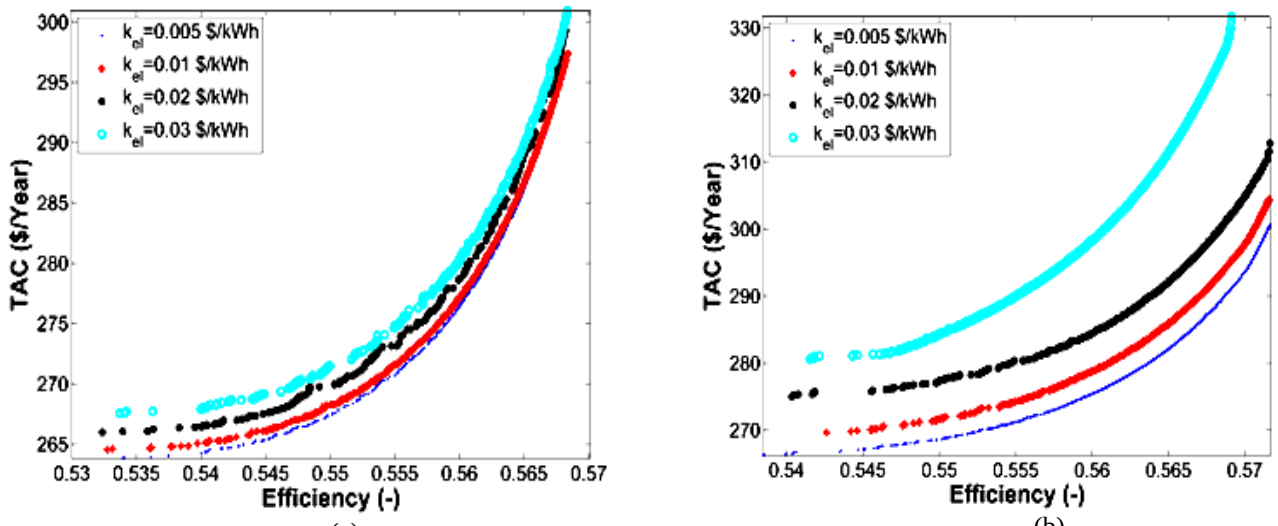

(a) (b)

Fig. 6. Optimum Pareto fronts for different electricity price and tube geometries
a. Collector with plain tube, b. Collector with DST tube

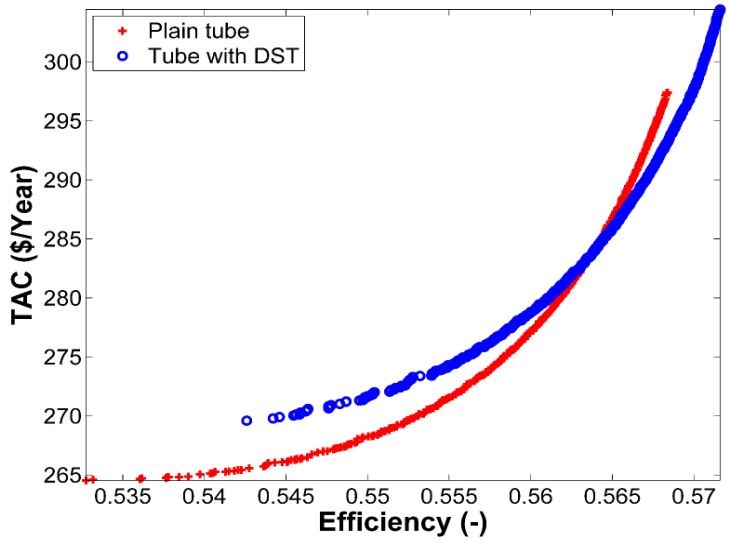

(a)

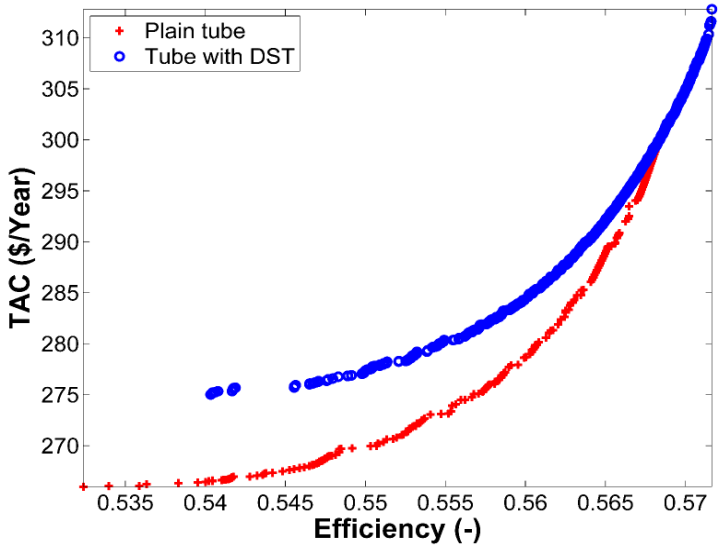

(b)

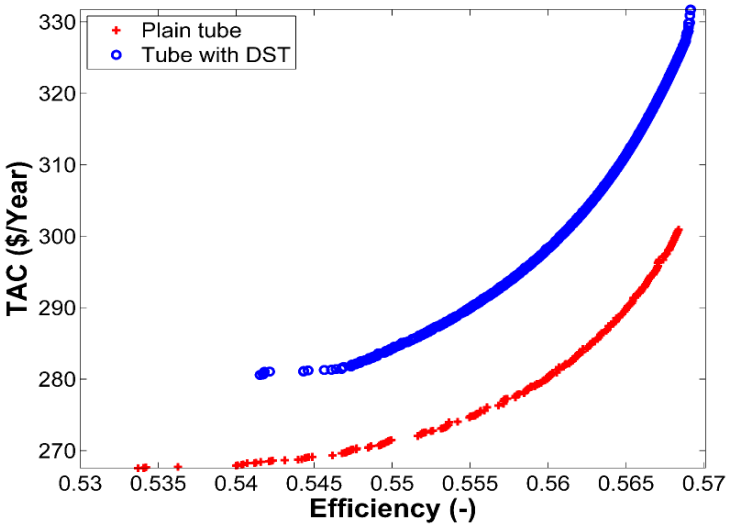

(c)

Fig. 7 Optimum Pareto fronts for collector with different tube geometry and electricity price) a. k_{el}=0.01, b. k_{el}=0.02 and c. k_{el}=0.03 $ kWh-1

4. Conclusion

In this investigation, multi-objective optimization of FPSC considering tubes with DST has been successfully applied using the NSGA-II algorithm. Six design parameters were considered in the case of plain tube while two additional parameters were selected in the case of tube with DST (eight design parameters all together). The main goal of this paper was to simultaneously improve the FPSC efficiency and TAC and derive the Pareto optimal front. The findings showed the level of engagement in the two objective functions. Optimum results showed that, FPSC with tube fitted with DST is dominated over the results of plain tube for the efficiency higher than 0.5566 while plain tube is better thermos-economic trend for the efficiency lower than 0.5566. Furthermore, the higher maximum efficiency was detected in the case of DST while the lower TAC in the case of plain tube which show the advantage use of tube with DST for the application of FPSC with higher efficiency and advantage use of plain tube for the application of FPSC with lower cost. Finally, the optimization was carried out for the various prices of electrical energy. It was determined that each Pareto optimal front is completely controlled by the Pareto optimal front with the lower electricity price. It was observed that, by increasing the electricity price, the value of marginal efficiency increased and finally the tube with DST was not better than the plain tube for the all range of efficiency for the 0.03$kWh-1 as electricity price. On the other hand, a marginal efficiency was found for any cases with electricity prices lower than 0.03$kWh-1.

References

[1] Oyinlola MA, Shire G, Moss RW. Thermal analysis of a solar collector absorber plate with microchannels. Experimental Thermal and Fluid Science. 2015;67:102-9.

[2] Moravej M, Bozorg MV, Guan Y, Li LK, Doranehgard MH, Hong K, et al. Enhancing the efficiency of a symmetric flat-plate solar collector via the use of rutile TiO2-water nanofluids. Sustainable Energy Technologies and Assessments. 2020;40:100783.

[3] Dutta Gupta, K.K, Saha, S, Energy Analysis of Solar Thermal Collectors, Renewable energy and environment. 1990,33(1):283-287.

[4] Shojaeizadeh E, Veysi F, Yousefi T, Davodi F. An experimental investigation on the efficiency of a Flat-plate solar collector with binary working fluid: A case study of propylene glycol (PG)–water. Experimental Thermal and Fluid Science. 2014;53:218-26.

[5] Allouhi A, Amine MB. Heat pipe flat plate solar collectors operating with nanofluids. Solar energy materials and solar cells. 2021;219:110798.

[6] Montoya-Marquez O, Flores-Prieto JJ. The effect of the angle of inclination on the efficiency in a medium-temperature flat plate solar collector. Energies. 2017;10(1):71.

[7] Broekaert S, De Cuyper T, De Paepe M, Verhelst S. Evaluation of empirical heat transfer models for HCCI combustion in a CFR engine. Applied Energy. 2017;205:1141-50.

[8] Kang W, Shin Y, Cho H. Economic analysis of flat-plate and U-tube solar collectors using an Al2O3 nanofluid. Energies. 2017;10(11):1911.

[9] García-Guendulain JM, Riesco-Avila JM, Elizalde-Blancas F, Belman-Flores JM, Serrano-Arellano J. Numerical study on the effect of distribution plates in the manifolds on the flow distribution and thermal performance of a flat plate solar collector. Energies. 2018;11(5):1077.

[10] Khorasanizade H, Aghaei A, Ehteram H, Azimi A. Study and exergy optimization of a flat plate solar collector in a closed circuit utilized with reflectors and lenses using experimental results. Energy Engineering and Management. 2023;3(1):40-51.

[11] Hall III C, Glakpe E, Cannon J, Kerslake T. Thermodynamic analysis of space solar dynamic heat receivers with cyclic phase change. 1999.

[12] Mahanta D, Saha SK. Internal irreversibility in a water heating solar flat plate collector. Energy conversion and management. 2002;43(17):2425-35.

[13] Torres-Reyes E, Navarrete-Gonzalez J, Cervantes-de Gortari J. Thermodynamic optimization as an effective tool to design

solar heating systems. Energy. 2004;29(12-15):2305-15.

[14] Farahat S, Sarhaddi F, Ajam H. Exergetic optimization of flat plate solar collectors. Renewable energy. 2009;34(4):1169-74.

[15] Faizal M, Saidur R, Mekhilef S, Hepbasli A, Mahbubul I. Energy, economic, and environmental analysis of a flat-plate solar collector operated with SiO 2 nanofluid. Clean Technologies and Environmental Policy. 2015;17:1457-73.

[16] Harkouss F, Fardoun F, Biwole PH. Multi-objective optimization methodology for net zero energy buildings. Journal of Building Engineering. 2018;16:57-71.

[17] Jani D, Mishra M, Sahoo PK. A critical review on application of solar energy as renewable regeneration heat source in solid desiccant–vapor compression hybrid cooling system. Journal of Building Engineering. 2018;18:107-24.

[18] Zhou Y, Zheng S, Zhang G. Multivariable optimisation of a new PCMs integrated hybrid renewable system with active cooling and hybrid ventilations. Journal of Building Engineering. 2019;26:100845.

[19] Shafiey Dehaj M, Hajabdollahi H. Multi-objective optimization of hybrid solar/wind/diesel/battery system for different climates of Iran. Environment, Development and Sustainability. 2021;23(7):10910-36.

[20] Hajabdollahi H, Shafiey Dehaj M. Optimization of vapor compression refrigeration cycle considering a binary mixture of working fluids using evolutionary algorithms. Energy Equipment and Systems. 2021;9(1):91-106.

[21] Bezaatpour M, Rostamzadeh H. Design and evaluation of flat plate solar collector equipped with nanofluid, rotary tube, and magnetic field inducer in a cold region. Renewable Energy. 2021;170:574-86.

[22] Qiu G, Ma Y, Song W, Cai W. Comparative study on solar flat-plate collectors coupled with three types of reflectors not requiring solar tracking for space heating. Renewable Energy. 2021, 1;169:104-16.

[23] Mohan S, Dinesha P, Iyengar AS. Modeling and analysis of a solar minichannel flat plate collector system and optimization of operating conditions using particle swarms. Thermal Science and Engineering Progress. 2021, 1;22:100855.

[24] Majumdar R, Saha SK, Patki A. Novel dimension scaling for optimal mass flow rate estimation in low temperature flat plate solar collector based on thermal performance parameters. Thermal Science and Engineering Progress. 2020, 1;19:100569..

[25] Sheikholeslami M, Farshad SA, Ebrahimpour Z, Said Z. Recent progress on flat plate solar collectors and photovoltaic systems in the presence of nanofluid: a review. Journal of Cleaner Production. 2021, 15;293:126119.

[26] Verma SK, Sharma K, Gupta NK, Soni P, Upadhyay N. Performance comparison of innovative spiral shaped solar collector design with conventional flat plate solar collector. Energy. 2020, 1;194:116853..

[27] Hajabdollahi H. Thermoeconomic assessment of integrated solar flat plat collector with cross flow heat exchanger as solar air heater using numerical analysis. Renewable Energy. 2021, 1;168:491-504.

[28] Vengadesan E, Senthil R. A review on recent developments in thermal performance enhancement methods of flat plate solar air collector. Renewable and Sustainable Energy Reviews. 2020, 1;134:110315.

[29] Ganjehkaviri A, Jaafar MM. Multi-objective particle swarm optimization of flat plate solar collector using constructal theory. Energy. 2020, 1;194:116846.

[30] Karki S, Haapala KR, Fronk BM. Technical and economic feasibility of solar flat-plate collector thermal energy systems for small and medium manufacturers. Applied Energy. 2019, 15;254:113649.

[31] Visa I, Moldovan M, Duta A. Novel triangle flat plate solar thermal collector for facades integration. Renewable Energy. 2019, 1;143:252-62.

[32] Ma Q, Ahmadi A, Cabassud C. Optimization and design of a novel small-scale integrated vacuum membrane distillation-solar flat-plate collector module with heat recovery strategy through heat pumps. Desalination. 2020, 15;478:114285.

[33] Hajabdollahi M, Shafiey Dehaj M, Hajabdollahi H. Investigation of optimization algorithms and their operating

parameters in different types of heat exchangers. Energy Equipment and Systems. 2021, 1;9(4):351-70.
[34] Hajabdollahi H, Shafiey Dehaj M. Optimization of energy systems using the concept of balance in the nature. Environmental Science and Pollution Research. 2021;28(28):37580-91.
[35] Cetina-Quiñones AJ, Xamán J, Bassam A, Soberanis ME, Perez-Quintana I. Thermo-economic analysis of a flat solar collector with a phase changing material under tropical climate conditions: Residential and industrial case. Applied Thermal Engineering. 2021, 5;182:116082.
[36] Deng J, O'Donovan TS, Tian Z, King J, Speake S. Thermal performance predictions and tests of a novel type of flat plate solar thermal collectors by integrating with a freeze tolerance solution. Energy Conversion and Management. 2019, 15;198:111784.
[37] Balaji K, Kumar PG, Sakthivadivel D, Vigneswaran VS, Iniyan S. Experimental investigation on flat plate solar collector using frictionally engaged thermal performance enhancer in the absorber tube. Renewable Energy. 2019, 1;142:62-72.
[38] Anirudh K, Dhinakaran S. Numerical study on performance improvement of a flat-plate solar collector filled with porous foam. Renewable Energy. 2020, 1;147:1704-17.
[39] Hajabdollahi H, Shafiey Dehaj M, Aien M. Thermal and economic modeling and optimization of solar-assisted underfloor heating system considering hourly analysis. Journal of Thermal Analysis and Calorimetry. 2022;147(21):12079-92.
[40] Hajabdollahi H, Khosravian M, Dehaj MS. Thermo-economic modeling and optimization of a solar network using flat plate collectors. Energy. 2022, 1;244:123070..
[41] Dhairiyasamy R, Rajendran S, Khan SA, Alahmadi AA, Alwetaishi M, Ağbulut Ü. Enhancing thermal efficiency in flat plate solar collectors through internal barrier optimization. Thermal Science and Engineering Progress. 2024, 1;54:102856.
[42] Ghalati AS, Maleki A, Besharati S, Zarein M. Prediction and optimization of performance parameters of solar collectors with flat and porous plates using ANN and RSM: Case study of Shahrekord, Iran. Case Studies in Thermal Engineering. 2024, 1;60:104719..
[43] Ojeda JA, Esparza C, Méndez F. Optimizing solar collector through constructal design of Y-shaped networks with power-law nanofluid flow. Applied Thermal Engineering. 2024, 15;257:124465.
[44] Li ZY, Gong JH, Wang J, Lund PD. Optimizing research on flat-plate solar collector based on field synergy theory. Energy Reports. 2024, 1;12:1977-86.
[45] Kalogirou SA. Solar energy engineering: processes and systems. Elsevier; 2023.
[46] Foster R, Ghassemi M, Cota A. Solar energy: renewable energy and the environment. CRC press; 2009.
[47] Hay, J.E., Davies, J.A., 1980. Calculation of the solar radiation on an inclined surface. Proceedings of the first Canadian Solar Radiation Data Workshop, pp. 59.
[48] Shafiey Dehaj M, Zamani Mohiabadi M. Experimental study of water-based CuO nanofluid flow in heat pipe solar collector. Journal of Thermal Analysis and Calorimetry. 2019, 30;137:2061-72.
[49] Hajabdollahi Z, Hajabdollahi H. Thermo-economic modeling and multi-objective optimization of solar water heater using flat plate collectors. Solar Energy. 2017, 1;155:191-202.
[50] Lee PS, Garimella SV, Liu D. Investigation of heat transfer in rectangular microchannels. International journal of heat and mass transfer. 2005, 1;48(9):1688-704.
[51] Duffie John A, Beckman William A. Solar engineering of thermal processes. Wiley, New York. 1991.
[52] Mitchell JW. Heat transfer from spheres and other animal forms. Biophysical Journal. 1976, 1;16(6):561-9.
[53] Hollands K, Unny T, Raithby G, Konicek L. Free convective heat transfer across inclined air layers. 1976.
[54] Eiamsa-ard S, Promvonge P. Thermal characterization of turbulent tube flows over diamond-shaped elements in tandem. International Journal of Thermal Sciences. 2010;49(6):1051-6.
[55] Said Z, Sajid MH, Alim MA, Saidur R, Rahim NA. Experimental investigation of the thermophysical properties of AL2O3-

nanofluid and its effect on a flat plate solar collector. International communications in heat and mass transfer. 2013;48:99-107.

[56] Deb K, Agrawal S, Pratap A, and Meyarivan, T. A Fast and Elitist Multi-Objective Genetic Algorithm: NSGAII. IEEE Trans. Evolutionary Computation. 2002,6: 182–197.

[57] Mahmoodabadi M, Taherkhorsandi M, Safikhani H. Modeling and hybrid Pareto optimization of cyclone separators using group method of data handling (GMDH) and particle swarm optimization (PSO). International Journal of Engineering, Transactions C. 2013;26(9):1089-102